https://doi.org/10.5194/ar-2026-32
Preprint. Discussion started: 22 September 2026

AEROSOL Research Discussions

Chemical composition of indoor and outdoor particles in a building near an international airport: Influence of local and long-range transported air pollution.

Sami D. Harni[1], Delun Li[1], Ville Silvonen[2], Laura Salo[2], Teemu Lepistö[2], Toni Tykkä[1], Mohamed Elsayed[3], Luis Barreira[1], Sanna Saarikoski[1] Ilpo Kulmala[4], Jarkko V. Niemi[5], Heidi Hellén[1], Arto Säämänen[4], Topi Rönkkö[2], Hilkka Timonen[1]

[1]Atmospheric Composition Research, Finnish Meteorological Institute, PL 503, FIN-00101 Helsinki, Finland
[2]Aerosol Physics Laboratory, Physics Unit, Faculty of Engineering and Natural Sciences, Tampere University, Tampere, Finland
[3]Department of Civil Engineering, Faculty of Built Environment, Tampere University, Tampere, Finland
[4]Clean Air Solutions, Built Environment and Mobility, VTT Technical Research Centre of Finland Ltd., Tampere, Finland
[5]Helsinki Region Environmental Services Authority HSY, FI- 00240 Helsinki, Finland

Correspondence to: Sami Harni (sami.harni@fmi.fi)

Keywords: indoor aerosol, black carbon, aerosol composition, long-range transport, ventilation

To be submitted to: Aerosol Research

Abstract.

Atmospheric pollution poses a significant threat to human health. These effects on human health are well documented in outdoor environments. However, in the Western world, people currently spend most of their time indoors. Therefore, studying the relationship between outdoor and indoor pollutant concentrations is essential. In this study, outdoor and indoor concentrations were measured in an unoccupied, mechanically ventilated building in Finland equipped with air-filtration and heat-recovery systems. Sampling was performed using a switching valve system that alternated sampling location between the building's air intake before filtration and the exhaust air vent, enabling near-simultaneous measurement of indoor and outdoor pollutant concentrations. The measurement campaign was conducted between 13th and 27th of February 2025. During the measurement period, a strong long-range transport (LRT) episode was observed, providing a good opportunity to study the effects of LRT on indoor pollutant concentrations. The measured variables included the chemical composition of aerosol particles, black carbon concentration, particle mass and number concentrations, and particle size distributions. Also, the effect of the nearby airport on the pollutant concentrations was discussed. The airport was found to have a large effect on particle number concentrations but almost no effect on particle mass or black carbon concentrations. The most abundant chemical component of aerosol particles both indoors and outdoors was organic matter. However, outside, the second most abundant component was nitrate, while indoors, more sulfate was measured. For the measured variables, the indoor-outdoor (I/O) ratios were calculated under normal and LRT conditions. Most of the I/O ratios remained stable between normal and LRT conditions.

https://doi.org/10.5194/ar-2026-32
Preprint. Discussion started: 22 September 2026

Exceptions to this were particulate matter and black carbon concentrations, which had higher I/O ratios during normal conditions, while particle number concentration had notably higher I/O ratios during LRT. The notably higher IO ratio of particle number concentrations was most likely due to the increase in the geometric mean diameter of particles. Notably, the ratios varied between the different measured components. The lowest I/O ratio of 0.20 ± 0.08 was observed for nitrate during the LRT. The low I/O ratio of nitrate might be related to the increasing temperature of aerosol particles while being transported indoors and therefore to increased evaporation. Under LRT conditions, the indoor black carbon concentrations increased to levels similar to those at street canyon measurement sites in Finland. The nearby airport was found to have a notable effect on the particle number but not particle mass concentrations or BC concentrations.

1 Introduction

The negative effects of aerosol pollution on human health and the environment are well-established (Shalini V. et al., 2023). Therefore, outdoor pollution concentrations in urban environments have been extensively studied (Colbeck & Lazaridis, 2010; Norra et al., 2023; Robinson et al., 2018; Wu & Boor, 2021). However, especially in the Western world, humans spend almost 90% of their time indoors (Matz et al., 2014). Therefore, it is increasingly important to expand the focus of aerosol pollution studies to indoor air and investigate how outdoor pollution affects indoor pollutant levels to enable a detailed characterisation of outdoor-to-indoor transport and the evaluation of the health effects associated with different pollution sources. The near-simultaneous characterisation of aerosol chemical composition indoors and outdoors is also rarely researched (Garbarienė et al., 2022; Talbot et al., 2017). The transport of outdoor pollutants indoors is highly dependent on the pollutant in question and the type of building (Deng et al., 2015; Johnson et al., 2016; Krebs et al., 2021). In the absence of indoor sources, particulate matter (PM) concentrations are typically lower inside compared to outdoors (Bucur & Danet, 2019; Franck et al., 2003). However, some pollutants behave differently; for example, some volatile organic compounds (VOCs) have been shown to have higher concentrations indoors (Rumchev et al., 2007). Despite the differing concentrations and pollution sources, the indoor and outdoor concentrations appear to be strongly but variably correlated. For example, Santiago et al. (2022) reported that the relationship between pollutant concentrations indoors and outdoors was 0.56 ± 0.24. Krebs et al. (2021) found that a 10% increase in the outdoor PM concentrations was associated with a 4.2-6.1 % increase in indoor PM concentrations.

The change in aerosol concentrations during outdoor-to-indoor transportation is affected by numerous mechanisms. For example, aerosol heating while being transported indoors has been shown to reduce the indoor-outdoor ratios (I/O) of some compounds and particle size, whereas coagulation has been shown to reduce the aerosol particle number concentrations indoors (Johnson et al., 2016; Talbot et al., 2017; Vu et al., 2017). In addition to the aerosol-related parameters, the relationship between indoor and outdoor air pollutant concentrations depends on characteristics of the studied building, and therefore, indoor-outdoor relationships cannot be generalised, as it is dependent on building systems (Saksena & Uma, 2008). For example, reported that the number of open windows and how high the room is located compared to the ground level affected indoor concentrations, with higher elevations corresponding to lower indoor concentrations (Santiago et al., 2022). In addition, the

https://doi.org/10.5194/ar-2026-32
Preprint. Discussion started: 22 September 2026

AEROSOL Research Discussions

ventilation type affects the relationship between indoor and outdoor concentrations (Park et al., 2014). Ventilation in buildings can be arranged in three different ways: either using natural ventilation, mechanical ventilation, or hybrid ventilation (Olstrup et al., 2021). In general, mechanically ventilated buildings tend to have lower indoor particle concentrations than naturally ventilated buildings, although this effect depends on filtration efficiency, leaks, and system operation (Park et al., 2014). In mechanically ventilated buildings, filter type also affects the pollutant transport from outdoors to indoors, with different filters showing different efficiencies in different particle size ranges (Karjalainen et al., 2017).

In this study, the chemical composition and number concentration of indoor and outdoor particles were measured in a meeting-hall-type building, Aviapolis X, in Helsinki, Finland. Additionally, I/O ratios were determined to study the relationship between indoor and outdoor concentrations for the different PM constituents. Aviapolis X was a mechanically ventilated space with an intake air filtration system with a filter class of ePM_1 60% (removing at least 60% of 0.3 to 1 µm sized particles). The building had no additional indoor activities during the measurement period. The building was located near the Helsinki-Vantaa airport, with the nearest runway located 1.3 km in the north-west direction. To the knowledge of the authors, transportation of atmospheric pollutants indoors has not been studied this close to an airport before. Additionally, there are two busy highways on the east and south sides at a distance of less than 2 km. During the measurement campaign, a strong long-range transport (LRT) event was observed in the area, providing a rare opportunity to investigate the effects of LRT events on indoor pollutant concentrations. As a reference, Niemi et al. (2009) reported 40 LRT events exceeding a 24-h mean peak $PM_{2.5}$ concentration of 25 µg m^{-3} from 1999 to 2007. The primary aim of the measurements was to study how local outdoor pollution sources affect the gas and particulate matter concentrations and compositions in indoor and outdoor environments.

2 Experimental

2.1. Measurement location and building characteristics

Measurements were conducted between the 13th and 27th of February 2025 at the Aviapolis X building, which is a temporary pavilion designed for exhibitions, events, and conferences. It is a single-story, wood-element, relocatable structure. The building has a total area of 163.5 square meters and a volume of 736 cubic meters. The foundation comprised steel base plates, and a load-bearing frame was constructed using cross-laminated timber (CLT). An open meeting room covered most of the floor area. Additionally, the building included a small kitchen, two toilets, and a storage area where the technical systems of the building were located. The building is located close to the Helsinki-Vantaa airport (~1 km) and two major highways (< 2 km). The airport has been identified as a major source of ultrafine particle pollution in the studied area (Lepistö et al., 2026). The location of the building is shown in Supplement S1. Together, the runways covered all angles between 270° and 90 ° with the nearest being located 1.3 km northwest of the site. The studied building was also in the vicinity of two major highways: E18 in the south at a distance of approximately 1 km and Highway 45 in the east at a distance of approximately 2 km. These roads have traffic amounts of 93000 and 54000 vehicles/day for workdays and 60000 and 35000 cars/day for weekends, respectively (DigiTraffic). The traffic diurnal profiles are presented in Supplement S2.

https://doi.org/10.5194/ar-2026-32
Preprint. Discussion started: 22 September 2026

The building featured a mechanical supply and exhaust ventilation system. Heating and cooling were provided by heat pump technology, with heat distributed to spaces through air-heating systems. The heating, ventilation, and air conditioning (HVAC) system was operated in a constant air volume mode, day and night, throughout the measurement campaign. Fresh outdoor air was supplied at a rate of 500 L/s, and the extract air was expelled at a rate of 350 L/s. The airflow rates were measured using a hot-wire anemometer from the supply and extraction air ducts. The estimated uncertainty using this method was ±15%. The supply air filters were of the ePM_1 60% class, which is typical for this type of building. The ventilation airflow rates remained unchanged during the campaign, and the ventilation rate was maintained at 2.4 air changes per hour. This indicates that the building was over-pressurised most of the time because the intake airflow was 150 L/s larger than the extracted airflow. The measured air leakage rate q_{50} of the building envelope was quite high at 8.1 $m^3/h \cdot m^2$. The high envelope leakage rate resulted in wind-induced infiltration during windy conditions, enabling the transport of unfiltered outdoor air indoors.

2.2 Measurement setting

Sampling was performed using a valve system that alternated the sampling locations between the building air intake and exhaust every 15 min. Therefore, two periods of indoor air and two periods of outdoor air were sampled hourly. Hourly averages were calculated for both indoor and outdoor concentrations using one set of instruments. The concentrations and particle size distributions of the chemical components of the submicron particles were measured using a soot particle aerosol mass spectrometer (SP-AMS, Aerodyne; (Jayne et al., 2000; Onasch et al., 2012)) with a time resolution of 1 min. The SP-AMS data were analysed using the SQUIRREL TOF-AMS analysis toolkit 1.66 G, PIKA TOF-AMS HR Analysis 1.26 G, and WaveMetrics Igor Pro 8. The particle number and mass size distributions of particles 16 nm- 1 µm in size were measured using an electrical low-pressure impactor (ELPI+; (Järvinen et al., 2014)). In the data analysis, we assumed that the particles were spherical and of unit density. The ELPI+ filter stage was excluded from the analysis, as we discovered our measurement activity influenced sub-10 nm particles in the indoor air, which we wished to exclude from the analysis. The second stage had a lower cut-off size of 16 nm. BC concentrations were measured using two different methods: equivalent black carbon (eBC) measured with light absorption analysis and refractive black carbon (rBC) measured using laser-induced incandescence with SP-AMS. The eBC concentrations were measured using an aethalometer (AE36s, Magee Scientific) with a PM_1 cyclone to remove coarse particles. The eBC concentrations have been reported to be 2.7 – 3.1 times higher than those of rBC (Sharma et al., 2017). The AE36s data were also utilised to calculate the absorption Ångström exponent (AAE) of the measured aerosol based on the attenuation of light at wavelengths of 470 nm and 950 nm:

$$\mathrm{AAE} = -\frac{\ln {}^{b_{\mathrm{abs}}(470\ nm)}/_{b_{\mathrm{abs}}(950\ nm)}}{\ln \frac{470\ nm}{950\ nm}}, \qquad \text{(Eq.1)}$$

where b_{abs} is the aerosol light absorption coefficient, which is determined by measuring the attenuation of light. Notably, SP-AMS data were available only for February 20–27, whereas AE36s and ELPI+ data were available throughout the entire measurement period, from February 13 to 27. A schematic of the measurement system is shown in Supplement S3. The outdoor air sample was collected from the intake air before the filtration and heating system, and the indoor air sample was collected

https://doi.org/10.5194/ar-2026-32
Preprint. Discussion started: 22 September 2026

from the exhaust duct of the ventilation system of the building. To ensure that the instruments did not affect the measured concentrations, the exhaust from the instruments was led to the exhaust duct after the sampling point for the indoor air.

One of the major goals of this work was to measure the indoor-outdoor (I/O) ratios. The I/O ratio is defined as the indoor concentration divided by the outdoor concentration. In this study, the I/O ratios were calculated by dividing the hourly averaged pollutant concentrations of the incoming air by the pollutant concentrations sampled from the exhaust air.

2.3 Measurement of air filter filtration efficiency

Filtration efficiency for the ePM_1 60% particle air filter (600 mm x 600 mm) installed in the Aviapolis X building's HVAC system was evaluated in a laboratory setting after the measurement campaign. Efficiency was assessed by measuring the aerosol size distribution using two instruments: the PMS LAS-X II optical particle size analyser and the TSI Nanoscan SMPS 3910, by alternating upstream and downstream measurements of the filter. In accordance with the EN 16890-2 standard, diethyl hexyl sebacate (DEHS) and potassium chloride (KCl) were used as the challenge aerosols. Measurements were performed using a dedicated test rig presented in the supplement S4. The testing maintained an air volume flow rate of 0.500 m^3/s, which matched the conditions of the Aviapolis HVAC system. DEHS aerosol droplets ranging in size from 100 to 4000 nm were generated by bubbling compressed particle-free air through DEHS liquid, and the resulting droplets were introduced into a mixing chamber before passing through the filter material. Similarly, an aqueous (KCl) solution produced aerosol particles smaller than 100 nm. The KCl particles were neutralised with an X-ray ioniser (Palas type XRC 049) before being injected into the mixing chamber.

2.4 General description of measurement period

A strong 5-day long-range transport (LRT) event was observed during the measurement period of this study. Therefore, the measurement period can be divided into three periods: before the LRT event, during the LRT event, and after the LRT event. Because the period after the LRT was short, it was meaningful to combine the data from normal atmospheric conditions before and after the LRT event. However, as the measurements were also altered between indoor and outdoor every 15 min, hourly averaged data were available for both outdoors and indoors for each hour. The data were split into indoor and outdoor data for normal conditions and for LRT events. Thus, the data included four different types of data: indoor and outdoor data for LRT and indoor and outdoor data for normal conditions. Following similar criteria as used by Teinilä et al. 2025; Timonen et al. 2018. The LRT period was determined based on the following criteria: First, the $PM_{2.5}$ level at the Luukki measurement station was required to exceed 5 $\mu g\ m^{-3}$ during the episode. The Luukki measurement station is a regional background (60.3144° N, 24.6847° E) measurement station operated by the Helsinki Regional Environmental Services Authority (HSY), that is located approximately 15 km east of the measurement site. The time series for Luukki $PM_{2.5}$ is shown in Supplement S5. The second criterion was that the outdoor SO_4 concentration needed to exceed 0.25 $\mu g\ m^{-3}$. The SO_4 time series is presented in Supplement S6. In addition to the concentration-based criteria, 72-h back trajectories at an altitude of 500 m were calculated using the

https://doi.org/10.5194/ar-2026-32
Preprint. Discussion started: 22 September 2026

NOAA HYSPLIT model during the entire measurement period at 8-h intervals to determine the origins of the air masses during the measurement campaign. Based on these criteria, the LRT event was defined to have started at noon on February 21st, 2025, and ended at 8 PM on February 26th. The LRT back trajectories are presented in Figure 1 for three time periods: before the LRT (blue), during the LRT (red), and after the LRT (black). The last trajectory of the normal period is presented as a dotted blue line, and the first back trajectory of the normal period after the LRT is marked with a black dotted line. In Figure 1, it is evident that before the defined start of the LRT, the air masses originated from the clean Arctic areas in the north. Therefore, the majority of the pollutants measured in these air masses were likely from local sources. At approximately noon on 21 February, when the conditions changed from normal to LRT (marked with a dotted blue line), the air masses began to arrive from over the Baltic countries and Poland. Subsequently, during the LRT event, air masses originated from middle and eastern Europe (marked in red). Again, on 26 February at 8 pm, the origin of the air masses changed (dotted black), and the air started to arrive from the North Sea over Sweden and remained there after the LRT (black).

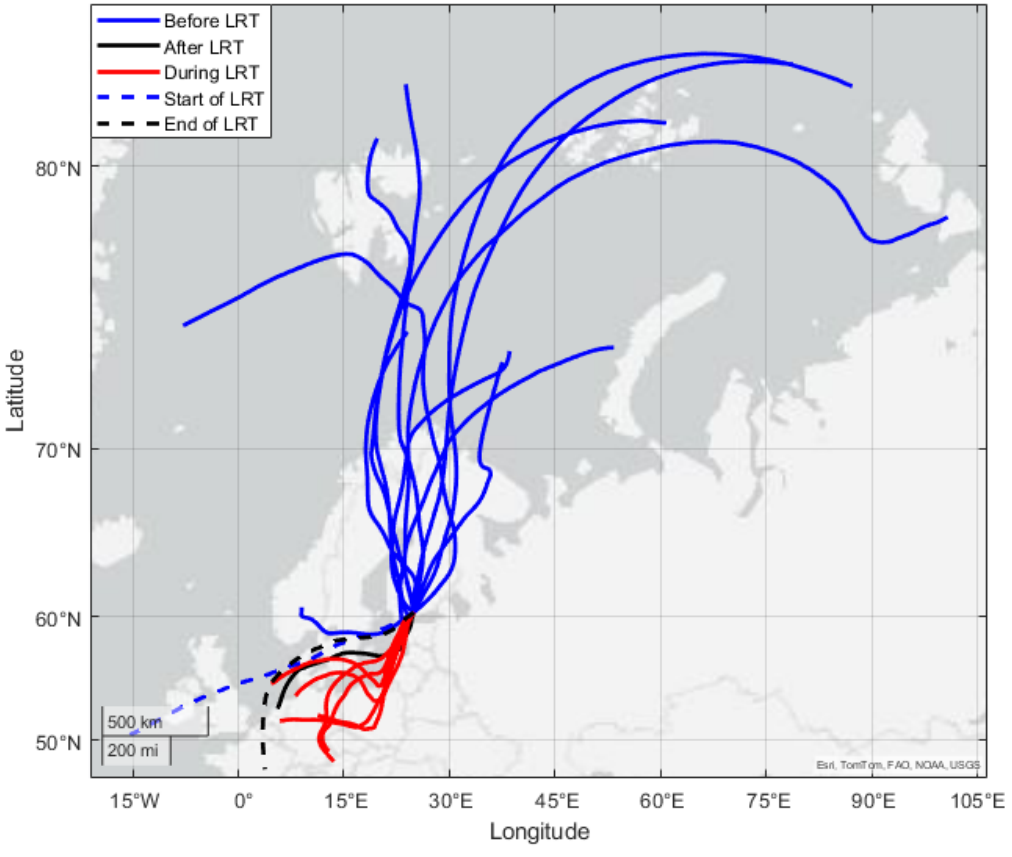

Figure 1: Calculated three-day (72 h) air mass back trajectories at an elevation of 500 m every 8 h before, during, and after the LRT episode. The blue lines mark the back trajectories before the start of the LRT episode. The dotted blue line marks the trajectory at the start of the LRT episode at 12 pm on 21 February. The red lines mark the trajectories during the LRT. The black

https://doi.org/10.5194/ar-2026-32
Preprint. Discussion started: 22 September 2026

dotted line indicates the air mass trajectory at the end of the LRT period. The black line indicates the back trajectory after the long-range transport (LRT) period. The dotted black line marks the end of the LRT period at 8 PM on February 26

The beginning of the LRT is clearly visible when inspecting the time series of the meteorological parameters presented in Supplement S7. The wind direction remained stable, coming from the south (approximately 180º), and the temperature remained stable at approximately 0 ºC during the entire LRT episode. Notably, temperature and wind direction were also similar during the short period of available SP-AMS data before and after the LRT episode. Therefore, analysing the influence of wind direction on the concentrations of chemical components measured with SP-AMS was not meaningful. Before the start of the LRT event, the variation in the meteorological parameters was larger, with wind directions covering all possible directions and hourly wind speed averages changing between 0 and 10 m s^{-1}. The ambient temperature varied between -15 and 0 °C. The RH was similar between the normal and LRT periods. During the LRT period, the wind speeds were the highest at the beginning and decreased thereafter.

3 Results and discussion

Figure 2 shows the particle number and mass concentrations as time series and the median particle size distributions during LRT and normal conditions. The LRT period was characterised by high mass concentrations, whereas the period preceding the LRT had a high particle number concentration because the winds originated from the airport during that time. Aircraft engines emit large amounts of small particles, especially in the particle size range below 23 nm. (Lepistö et al., 2026; Takegawa, 2023). In the number size distribution, it can be seen that the LRT episode has a particle mode at ~150 nm, whereas before and after the LRT episode, the modal size is below 50 nm. This mode of smaller particles did not disappear entirely during the LRT but was significantly diminished when the wind blew from the south. Like airports, road traffic is also a source of ultrafine particles, and highways were located south of the measurements. Particle emissions from road traffic are estimated to be around 10^{14} per kg of fuel, whereas airport-related particle emissions are estimated to be orders of magnitude larger, around 10^{15} to 10^{16} per kg of fuel (Li et al., 2026; Lintusaari et al., 2023; Voigt et al., 2026).

https://doi.org/10.5194/ar-2026-32
Preprint. Discussion started: 22 September 2026

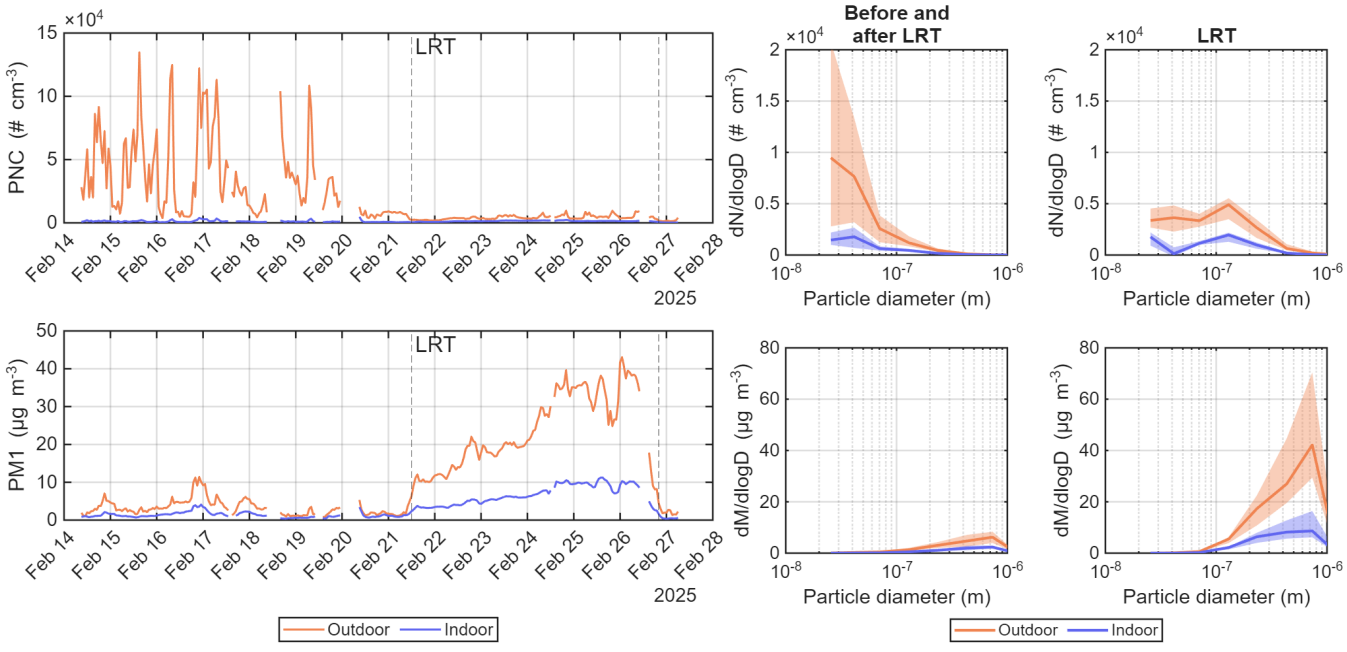

Figure 2: Time series and size distribution for the particle number and mass concentration for particle sizes of 16 nm to 1 µm, as measured with the ELPI+. The distributions are medians, with shaded areas representing the interquartile ranges.

The mean geometric size of outdoor particles over time is presented in Supplement S8 (a), and the influence of size on the infiltration of particles from outdoor air to indoor air in Supplement S8 (b). The percentage of particles infiltrating into indoor air increased substantially (from 2 % to 13 %) during the LRT episode, as the particles increased in size close to the most-penetrating particle size (see Supplement S9). The LRT episode also increased the mass median size, although not as dramatically, and the influence on mass infiltration was the opposite, with a slightly lower infiltration rate of 25 % (down from the initial 33 %). In terms of mass, the particles were close to the most-penetrating particle size to begin with and grew past it during the LRT. It is interesting to note that particle infiltration can simultaneously increase and decrease, depending on the measured metric.

Figure 3 presents the time series for the SP-AMS data separated into different components: organics (Org), sulfate (SO_4), nitrate (NO_3), ammonium (NH_4), refractory black carbon (rBC), and chloride (Chl) for outdoors (Panel A) and indoors (Panel B). Most of the available AMS data were measured during the LRT events. The change in concentration between outdoors and indoors was not the same for all chemical components; outdoors, NO_3 was the second most abundant component, whereas indoors, SO_4 was the second most abundant component after Org. This can also be observed in the I/O ratio time series (Figure 8C), where NO_3 had the lowest I/O ratio. Significant contributions of LRT to indoor aerosol concentrations have also been reported previously (Yli-Tuomi et al., 2008). During the LRT event, the concentrations increased steadily until noon on the 24th and remained elevated until noon on the 26^{th,} when the concentrations began to decrease. Interestingly, the I/O ratios of the different chemical components appeared to moderately correlate with wind speed during the LRT, with the strongest correlations (R-squared) of 0.59, 0.51, and 0.45 observed for NO_3, NH_4, and Org, respectively. The correlation of I/O-ratios

https://doi.org/10.5194/ar-2026-32
Preprint. Discussion started: 22 September 2026

with wind speed is presented in supplemental material S10. This could have been caused by the wind increasing the leakage through the building envelope, thereby slightly elevating the indoor concentrations during high wind speed conditions.

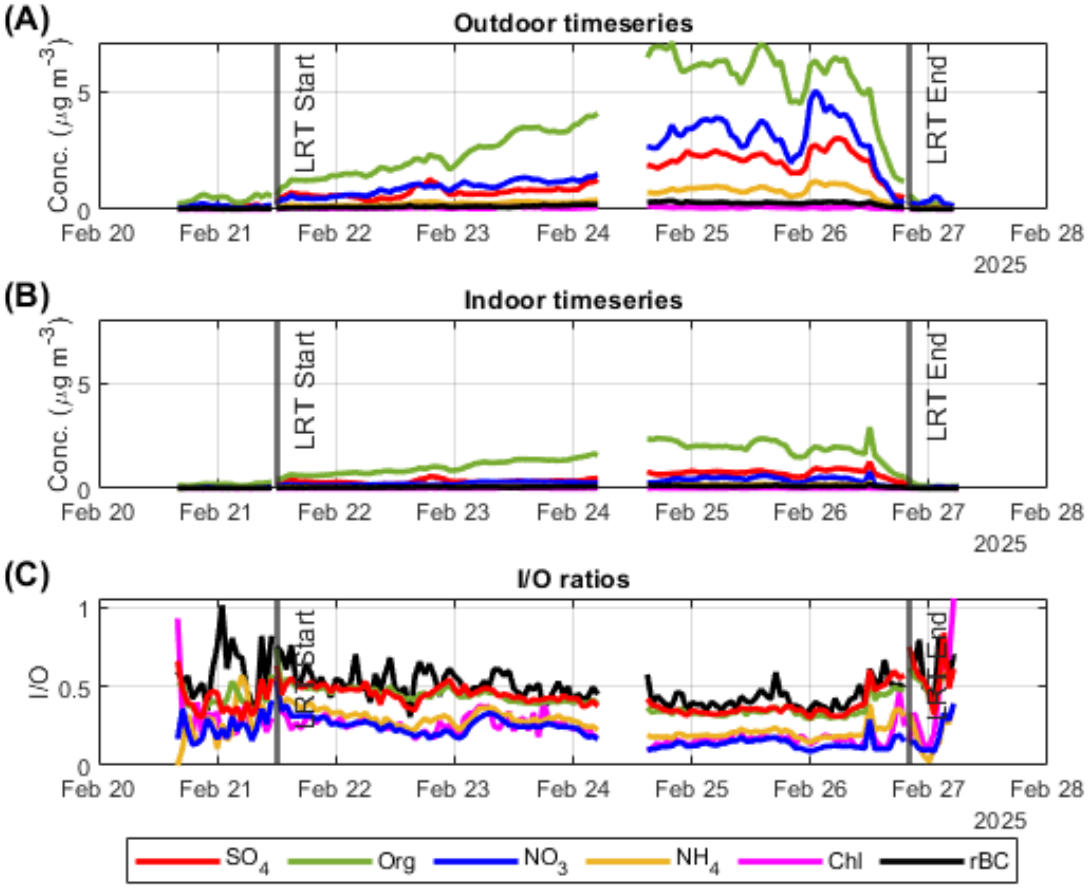

Figure 3: Time series of different chemical components of particles measured with SP-AMS: sulfate (SO_4), organics (Org), nitrate (NO_3), ammonia (NH_4), chloride (Chl), and refractory black carbon (rBC). Panels A and B represent time series of outdoor and indoor concentrations, respectively. The start and end of the long-range transport (LRT) event are indicated by black vertical lines. Panel C presents the indoor-outdoor (I/O) ratios corresponding to the concentration time series shown in panels A and B.

The I/O ratio time series calculated for the chemical compounds measured with SP-AMS is presented in Figure 3, panel C. The I/O ratio was more stable during the LRT event, likely because of elevated and more stable concentrations than under normal conditions. The highest I/O ratios were observed for rBC, SO_4, and Org, whereas NH_4, NO_3, and chloride had much lower I/O ratios. To inspect the I/O ratios for the different compounds more closely, the average I/O ratios are presented for different chemical components measured with SP-AMS: Chl, NH_4, NO_3, Org, SO_4, rBC, and eBC concentrations measured with AE36s (see Table 1). Here, the different I/O ratios between the pollutants were more apparent. One possible reason for different I/O ratios could be that pollutants were present at different particle sizes, as building ventilation effectiveness depends

https://doi.org/10.5194/ar-2026-32
Preprint. Discussion started: 22 September 2026

on particle size (Hanley et al., 1994; Karjalainen et al., 2017). The lowest I/O ratio was observed for NO_3, and overall, the highest was observed for rBC. However, it is important to note that the rBC and Chl concentrations were very low and therefore have a large uncertainty. Org and SO_4 also had notably higher I/O ratios than NO_3. Varying I/O ratios for different chemical components have also been observed in earlier studies, with NO_3 having lower I/O ratios than SO_4, NH_4, Org, and BC (Johnson et al., 2016). For some pollutants, PM_1, eBC, rBC and Chl, a slightly higher I/O ratio was observed during normal conditions compared to the LRT. However, for the rest, there were no significant differences between the normal and LRT conditions, and for PNC the I/O ratio was even higher during LRT. The I/O ratios remaining similar between pollution events and normal conditions have also been reported by Pauraite et al. (2021), who found that the I/O ratios remained stable during a strong wildfire smoke episode. This highlights the importance of outdoor pollutant concentrations, or, as in the case here, the importance of supply air filtration in buildings, when the aerosols are not produced locally and the possibility of reducing the outdoor concentrations is minimal.

Table 1: I/O ratios for different pollutants: PNC and PM_1 measured with ELPI+ with eBC, rBC, Chl, NH_4, NO_3, Org and SO_4 during the normal period (13.2.-21.2. 12 PM, 26.2. 8 PM-27.2.) and LRT (21.2. 12 PM- 26.2. 8 PM). Notably, the period of data available during the normal period before LRT was longer for eBC (AE36) and ELPI (13.-21.2.) than that for SP-AMS-related parameters (20.-21.2.).

		I/O	Average conc. outdoors	Average conc. indoors
ELPI+ PNC (cm^{-3})	Normal	0.07 ± 0.07	(32 ± 31)×10^3	(1.1 ± 0.7)×10^3
	LRT	0.34 ± 0.08	(4.3 ± 1.7)×10^3	(1.4 ± 0.4)×10^3
ELPI+ PM_1 ($\mu g\ m^{-3}$)	Normal	0.42 ± 0.14	3.2 ± 2.0	1.7 ± 0.7
	LRT	0.29 ± 0.03	23.6 ± 9.9	6.6 ± 2.6
eBC ($\mu g\ m^{-3}$)	Normal	0.43 ± 0.34	0.79 ± 0.77	0.27 ± 0.23
	LRT	0.29 ± 0.04	2.14 ± 0.89	0.62 ± 0.27
rBC ($\mu g\ m^{-3}$)	Normal	0.61 ± 0.17	0.03 ± 0.01	0.02 ± 0.01
	LRT	0.48 ± 0.10	0.19 ± 0.09	0.08 ± 0.03
Chl ($\mu g\ m^{-3}$)	Normal	0.33 ± 0.23	0.011 ± 0.004	0.0029 ± 0.001
	LRT	0.22 ± 0.08	0.06 ± 0.03	0.01 ± 0.01
NH_4 ($\mu g\ m^{-3}$)	Normal	0.24 ± 0.14	0.04 ± 0.02	0.01 ± 0.01
	LRT	0.26 ± 0.07	0.48 ± 0.32	0.11 ± 0.05
NO_3 ($\mu g\ m^{-3}$)	Normal	0.22 ± 0.09	0.19 ± 0.12	0.04 ± 0.02
	LRT	0.20 ± 0.08	1.85 ± 1.30	0.30 ± 0.15
Org ($\mu g\ m^{-3}$)	Normal	0.45 ± 0.09	0.40 ± 0.16	0.17 ± 0.02
	LRT	0.41 ± 0.07	3.73 ± 2.01	1.39 ± 0.59
SO_4 ($\mu g\ m^{-3}$)	Normal	0.46 ± 0.14	0.11 ± 0.03	0.05 ± 0.03
	LRT	0.42 ± 0.08	1.31 ± 0.79	0.51 ± 0.24

https://doi.org/10.5194/ar-2026-32
Preprint. Discussion started: 22 September 2026

Figure 4 shows the average mass size distributions (MSDs) for different chemical compounds measured with SP-AMS separately indoors, outdoors, under normal conditions and during the LRT event. The particles exhibited relatively similar unimodal MSDs for all the components. Under normal conditions, the peak particle sizes of the MSDs were smaller, and the concentrations were lower. The difference in concentration between outdoors and indoors was clearly visible under both LRT and normal conditions. Exact evaluations of the shapes and modalities of MSDs under normal conditions are challenging because of the low concentrations, resulting in relatively high noise in the data. However, during the LRT, the mass concentrations were higher, and data were available for a longer period, resulting in better-defined MSDs for the different compounds, even under indoor conditions. As the aerosol was transported from outdoors to indoors, the particle size shifted to smaller values. Outdoors, the mode diameter was approximately 400–500 nm for all compounds, whereas indoors, it was < 400 nm. In Figure 4C, the concentrations are seen to decrease most at approximately 500 to 600 nm particle sizes, while the particles are transported from outdoors to indoors. However, it needs to be noted that SP-AMS measures particles with approximately 100% efficiency only in particle sizes between 60 and 600nm. This could also partly explain the slightly larger average particle size seen in Figure 2, where the highest PM_1 concentration is measured at around 700 nm during the LRT event.

https://doi.org/10.5194/ar-2026-32
Preprint. Discussion started: 22 September 2026

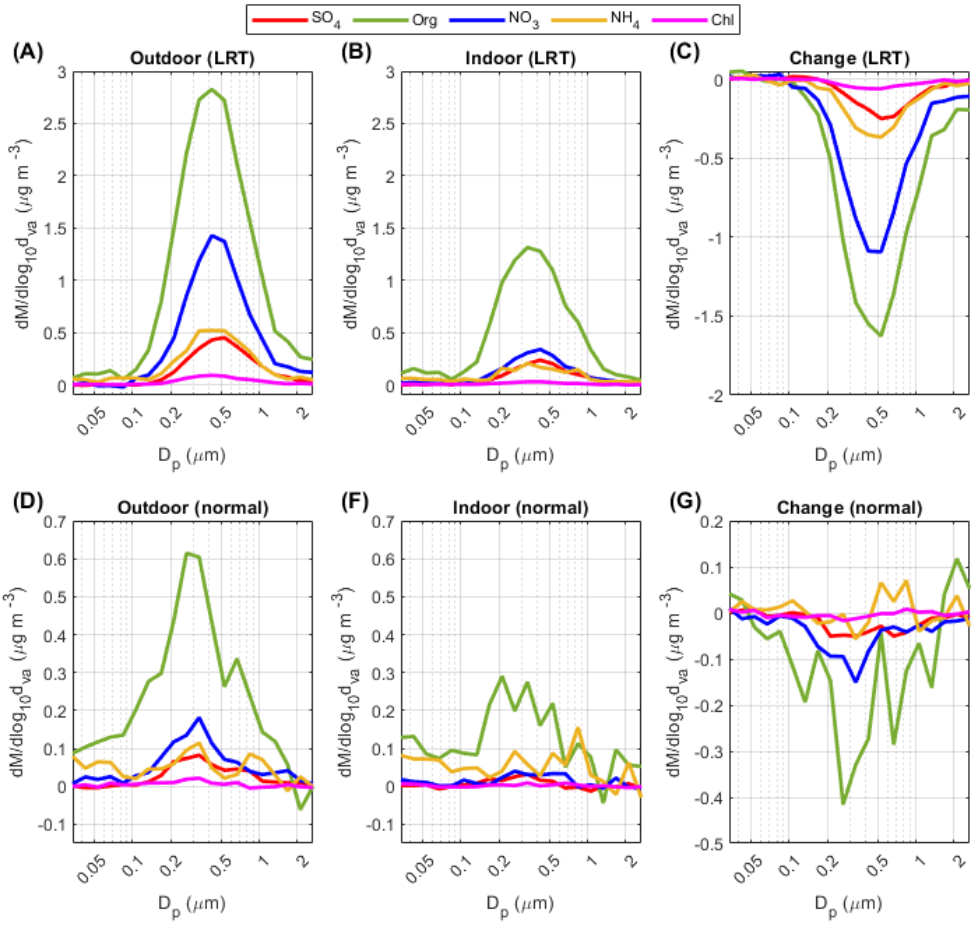

Figure 4: MSDs of the chemical components of aerosol particles measured with SP-AMS for Org in green, NO_3 in blue, NH_4 in orange, SO_4 in red, and Chl in purple separately for outdoors during LRT (A) and normal conditions (D), indoors during LRT (B), and normal conditions (F). The change caused by the transport of aerosol particles indoors (indoor MSD – outdoor MSD) during LRT is presented in panel (C), and that during normal conditions is presented in panel (G).

As the air intake flow exceeded the building air exhaust flow by 150 L s^{-1}, the building was over-pressurised during most of the measurement period. This was also observed in the continuous pressure difference measurements (see Fig. S11). Therefore, it was expected that almost all aerosol particles entering the building would pass through the filtration system in the air intake, and the filtration efficiency of the filter used in the building would significantly affect the reduction in pollutant concentration. The filtration efficiency of the filter used in the ventilation system as a function of particle size is shown in Figure S9. The filtration efficiency had a minimum value of 45 % for particle sizes between approximately 150 and 250 nm. By applying this filtration curve to the MSDs of outdoor concentrations, the indoor MSDs can in principle be attained if the only parameter affecting the indoor particle concentration is filtered outdoor concentrations, and the difference between estimated indoor concentration and outdoor concentration should be similar to the difference in measured concentrations shown in Figures 4C and 4G. Estimating indoor concentrations based on outdoor concentrations and knowledge of the filtration efficiency is useful

https://doi.org/10.5194/ar-2026-32
Preprint. Discussion started: 22 September 2026

when information is needed on a large number of buildings for the purposes of, e.g. exposure estimates. This estimation ignores potential other entry routes of pollution as well as indoor sources, deposition losses, condensation, evaporation, etc.

In Figure 5, the calculated MSDs from the filtration efficiency, measured MSDs, and differences between the measured indoor MSD and calculated indoor MSD are presented for the LRT period. The calculation was performed only on the LRT data, as low concentrations under normal conditions caused excessive noise. Panels A and B in Figure 5 show that the calculated and measured MSDs had different shapes. The measured MSDs were wider and included Org and NH_4 mass below 100 nm. However, in both cases, the mode particle diameter of Org was between 300 nm and 400 nm. Panel C of Figure 5 shows the differences between the measured and calculated MSDs for the different chemical components. Both positive and negative differences were observed. Notably, measured Org concentrations appeared to be higher across all particle sizes, measured SO_4 concentrations were higher at particle sizes above 100 nm, and measured NO_3 concentrations were notably lower between 150 and 700 nm in size. The fact that the measured Org and SO_4 concentrations exceeded the values calculated based on the theoretical filtration efficiency indicates that there were some internal sources for these pollutants, or, as the building was empty during the measurement, a more likely explanation is that, due to the high leakage rate of the building envelope, some outdoor concentrations might have penetrated indoors even when the building was mostly over-pressurised. The notably lower measured concentrations of NO_3 indicate additional mechanisms for NO_3 removal. NO_3 has been shown to be reduced more compared to the other compounds while being transported indoors, as also in other studies (Johnson et al., 2016; Miller et al., 2017; Sarnat et al., 2006). This could be caused by the volatile nature of NO_3. This has also been proposed by (Sarnat et al., 2006). One plausible removal mechanism for NO_3 is the transformation of ammonium nitrate to ammonia and nitric acid gases (Lunden et al., 2003). The filtration efficiency has been determined as a function of particle mobility size for particles below 100 nm and optical size for particles larger than 100 nm; thus, different filtration efficiencies could also be explained by differences in the average shape and density, which could affect their aerodynamic or optical size and hence affect the differences in filtration of different components.

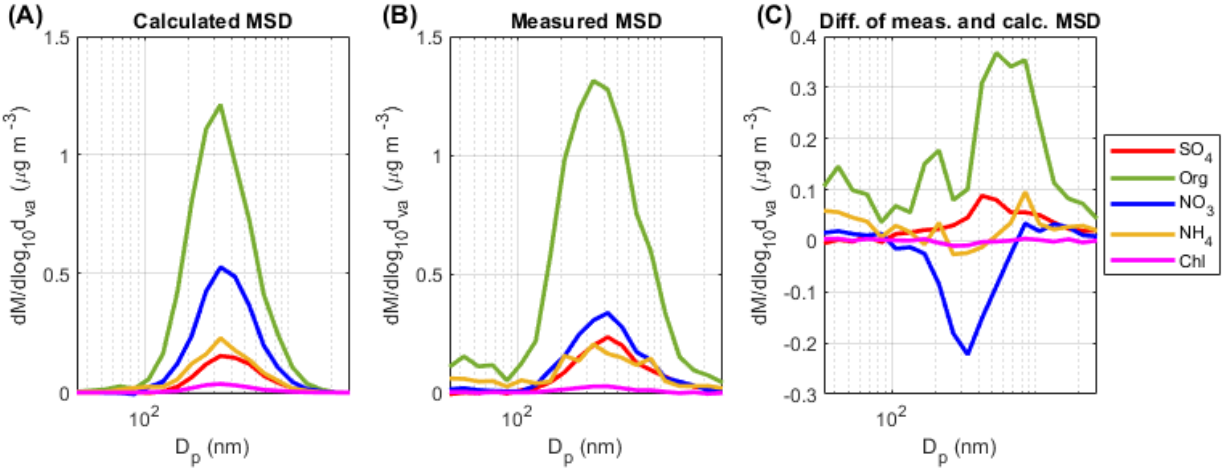

https://doi.org/10.5194/ar-2026-32
Preprint. Discussion started: 22 September 2026

AEROSOL Research Discussions

Figure 5: Panel A: MSDs of SO_4, Org, NO_3, NH_4, and Chl indoors during the LRT calculated using the filtration efficiency combined with SP-AMS data from outdoors. Panel B: The measured MSDs of the indoor aerosol components during LRT. Panel C: The differences between the measured and calculated MSDs for different chemical components indoors during LRT.

3.3 Black carbon

The time series of hourly averaged eBC measured with the AE36s is presented in Figure 6. The LRT event was clearly visible as consistently elevated concentrations. However, the highest concentration peaks were observed under normal conditions. These peaks were very high, exceeding 5 µg m^{-3}. For comparison, the yearly averages of traffic environments in Finland have varied between 0.4 and 0.8 µg m^{-3} (Korhonen et al., 2025). In addition, during the later part of the LRT event, the outdoor eBC concentrations were approximately 3 µg m^{-3}, exceeding the traffic environment averages by almost an order of magnitude, with indoor concentrations reaching 1 µg m^{-3} at that time. This is twice the annual average of BC at traffic locations (Korhonen et al., 2025). In addition, under normal conditions, during the highest peak, the indoor eBC concentrations exceeded 1 µg m^{-3}. Notably, in Figure 6, the two high peaks observed on Sunday, February 16th 6 pm to February 17^{th,} 2 am and Thursday, February 20^{th,} between 4 am and 10 am have a similar pattern: when the wind is blowing from southeastern directions, the concentrations increase, and when the wind direction turns more to the east, the concentrations start to fall. The different times of the peaks could indicate different sources: biomass burning for the first and traffic for the second peak. As the first peak is observed during weekend evening, that is the time when more wood is burned, and the second peak is observed during workday morning rush hours (Mohammadabadi et al., 2026). However, this was not supported by the biomass burning percentage calculated using the aethalometer model, which was 42% for both events in this study. Overall, it was evident that when the wind was blowing from the north, the eBC concentration was very low, indicating that the airport was not a large contributor to the BC concentrations. The low effect of airports on BC concentrations has also been reported in other studies (Lepistö et al., 2026; Masiol et al., 2016; Stacey et al., 2020). Durdina et al. (2017) have also shown that the mass-based BC emissions from aeroplanes are notably lower than estimated. In Figure 6, panel C, the I/O ratio time series for eBC is shown. There are significant peaks reaching I/O ratios greater than one. This indicates that during these periods, the indoor concentration exceeded the outdoor concentration. This does not seem to always be caused by the rapid decrease in elevated concentrations outdoors, with the change being slower inside the building because of a lower air exchange rate. Instead, these seem to occur when the concentration outdoors is very low; therefore, even low concentrations indoors may exceed the outdoor concentration, increasing the uncertainty in the accuracy of these peaks. Outside these peaks, the I/O ratio remained relatively stable at approximately 0.3.

https://doi.org/10.5194/ar-2026-32
Preprint. Discussion started: 22 September 2026

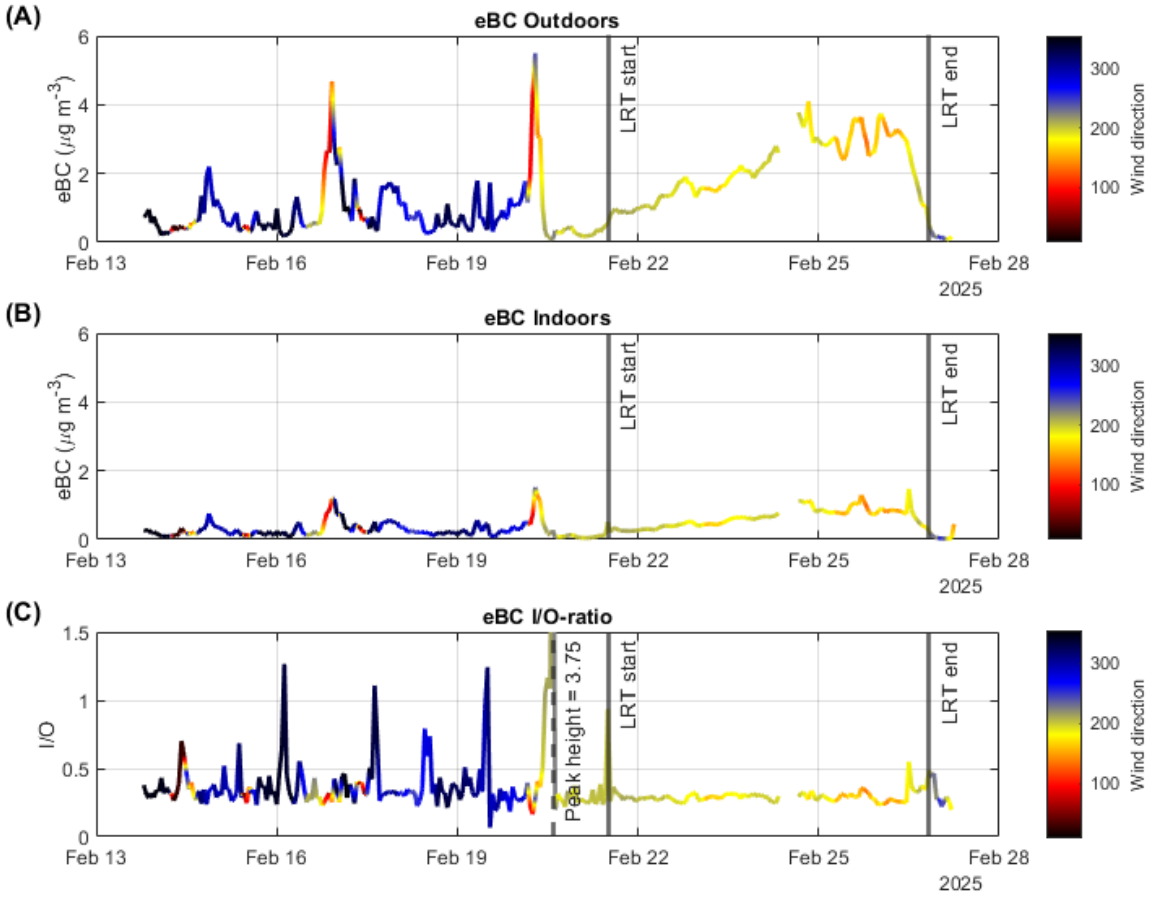

Figure 6: Panel (A) shows the outdoor and (B) indoor time series of the hourly equivalent black carbon (eBC). The start and end times of the long-range transport (LRT) event are indicated by the black vertical lines. The wind directions are indicated by colour bars. Panel (C) shows the time series of the I/O ratios calculated from outdoor and indoor time series. In panel C, the highest peak exceeding the limits of the figure is marked with a dotted vertical line.

Absorption measured with the aethalometer for nine different wavelengths, presented for different wind directions, indoors and outdoors, under normal and LRT conditions, is shown with the corresponding absorption ångstöm exponents (AAE) in Figure 7. The AAE is a measure of absorption dependency on the wavelength of light. This information from measurements of absorption at different wavelengths provides additional information about aerosols and is important regarding the climate effects of aerosols. Absorption at shorter wavelengths indicates the presence of brown carbon (Costabile et al., 2017), whereas the wavelength of 880 nm is referred to as BC. The ageing of atmospheric BC-containing aerosols has been shown to increase absorption at shorter wavelengths (Cappa et al., 2020). Notably, higher absorption at shorter wavelengths has also been related to biomass combustion, whereas absorption at longer wavelengths is related to fossil fuel combustion (Sandradewi et al., 2008). During LRT, the highest absorptions were measured at 370 nm, whereas under normal conditions, the highest absorption was

https://doi.org/10.5194/ar-2026-32
Preprint. Discussion started: 22 September 2026

measured at 370 nm only in one wind direction (135°–180°). In most cases, the highest absorptions were measured at slightly longer wavelengths (e.g. 400 or 470 nm). This indicates a more pronounced contribution of brown carbon to the aerosol during LRT and a more pronounced BC and traffic contribution during normal conditions. Under normal conditions, when the wind was blowing from 45° to 180°, there was a small difference between the highest and lowest absorption, and in some directions, such as 0–45° and 180–225°, the absorptions at all wavelengths were similar. During both normal and LRT conditions, the relative fractions of brown and black carbon appeared similar outdoors and indoors, indicating that filtration was similar for the two. However, the Ångström exponent was slightly higher for the LRT period. The strong wavelength dependence of light absorption has been linked to biomass combustion-produced aerosols (Kirchstetter et al., 2004). Therefore, higher absorptions were expected at shorter wavelengths during LRT. The higher eBC concentrations measured in the 45°–180° direction could indicate greater contributions from biomass combustion, as there are a significant number of detached houses with possible wood combustion in this direction. The AAEs were found to be higher during LRT and indoors compared to normal conditions and outdoors. The higher AAE during LRT was to be expected because of the longer atmospheric age of aerosols during LRT, as the AAE has been reported to be approximately 1.05 regardless of the particle size for fresh BC particles, and higher AAEs have been related to aged particles in particles larger than 0.12 µm (Liu et al., 2018). Regarding wind directions, the AAEs were largest when the wind was blowing between 135° and 270° and smallest when the wind was blowing between 315-90º.

https://doi.org/10.5194/ar-2026-32
Preprint. Discussion started: 22 September 2026

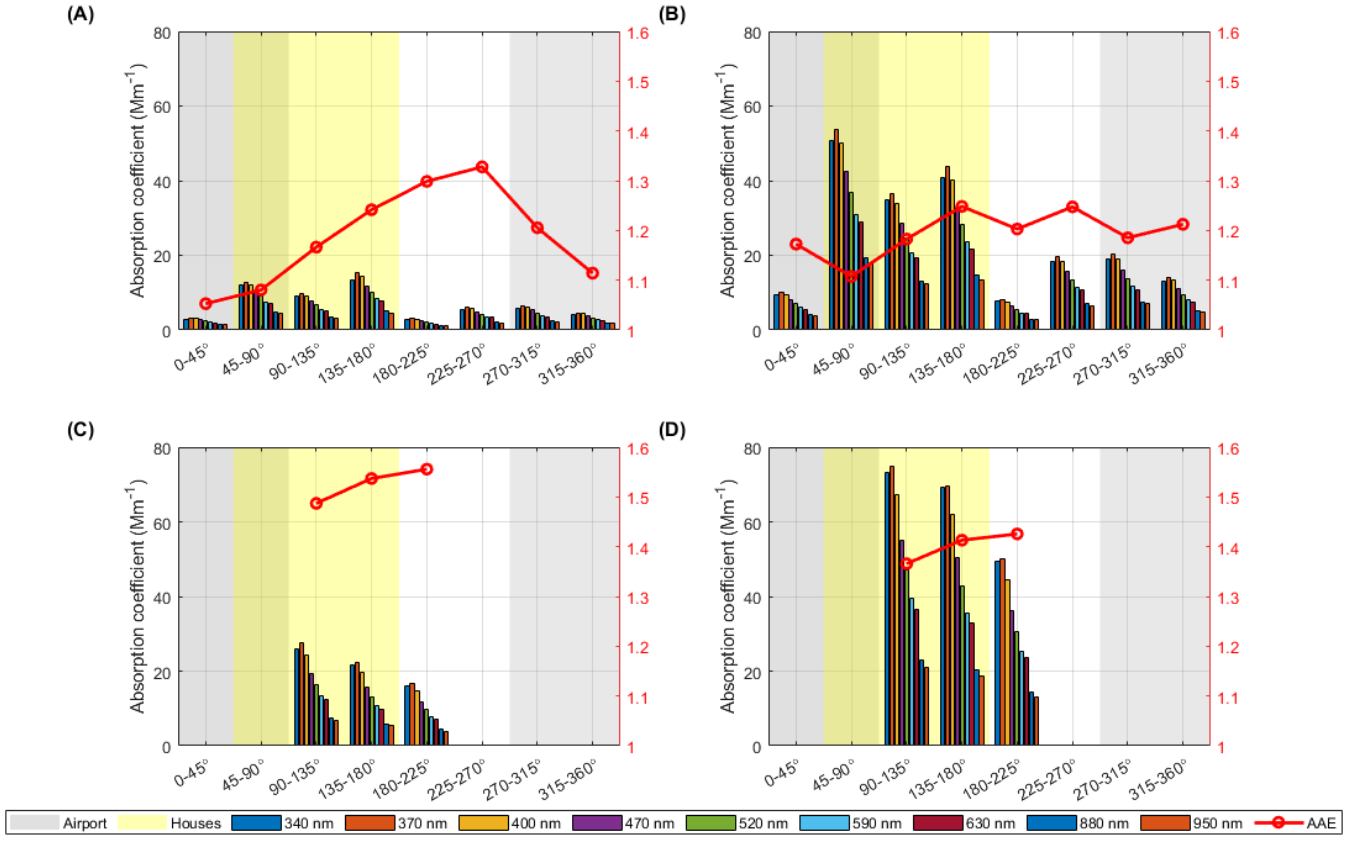

Figure 7: Equivalent black carbon (eBC) concentrations from different wavelengths from different wind directions indoors during normal conditions in panel A, outdoors during normal conditions in panel B, indoors during LRT in panel C and outdoors during LRT in panel D. The direction of the airport has been marked with figures on a grey background (270-90°) and nearby detached house areas with a yellow background (45-180°). Absorption Ångström exponents (AAE) have been plotted in figures with red lines.

4. Conclusions

In this study, a strong relationship was observed between outdoor and indoor pollutant concentrations. The results indicate that effective control of outdoor pollution is essential, even when populations spend most of their time indoors, as outdoor concentrations have a clear and significant contribution to indoor pollutant concentrations. An important factor affecting the indoor-outdoor ratios of pollutants was the filtration efficiency of the ventilation system. In this study, the building was overpressurised, and all incoming air passed through the filter (ePM_1 60%), thereby further increasing the significance of the filter efficiency. However, the relationship between indoor and outdoor pollutant concentrations was not the same for the different measured chemical compounds and also varied temporally. For some chemical components of aerosol particles, such as NO_3, the outdoor-to-indoor transport efficiency was lower than expected based on the filtration efficiency. This implies the presence of additional mechanisms for the loss of NO_3. Plausible mechanisms include the evaporation of NO_3 when the

https://doi.org/10.5194/ar-2026-32
Preprint. Discussion started: 22 September 2026

temperature increases during the transport of aerosols indoors. The immediate vicinity of a busy international airport did not seem to affect the BC concentrations, as the eBC concentrations were low when the wind was blowing from the airport. However, relatively high concentration peaks of eBC were measured at the site when the wind was blowing from the other directions toward the site. In addition to local sources, the long-range transport of air pollutants was seen to markedly influence indoor air quality, reinforcing the need for coordinated international action to improve air quality. Even under relatively clean conditions, such as in Finland, indoor concentrations can reach notable levels during LRT and other pollution events. For example, during LRT, the measured eBC concentrations were significant, and even the indoor concentrations exceeded typical yearly averages measured at a traffic site. For particulate matter, an interesting observation was made that during normal conditions, the I/O ratio for PNC was found to be only approximately one-sixth of the I/O for PM_1. During the LRT period, the I/O ratio increased for PNC and decreased for PM_1, resulting in a slightly higher I/O ratio for PNC than for PM_1. Also, airpost was observed to have a clear effect on PNC but not PM_1. This highlights that the changing conditions might have very different effects on the filtration efficiencies depending on the measured parameter.

Author contributions

SDH: Formal Analysis, Investigation, Data Curation, Writing – Original Draft, Visualisation

LS: Conceptualisation, Methodology, Formal Analysis, Investigation, Data Curation, Writing – Original Draft, Visualisation, Project Administration, Funding Acquisition

VS: Conceptualisation, Methodology, Investigation, Writing - review & editing

TL: Investigation, Formal Analysis, Writing – review & editing

IK: Investigation, Formal Analysis, Writing - review & editing

JVN: Conceptualisation, Project Administration, Writing - review & editing

AS: Conceptualisation, Investigation, Formal Analysis, Funding Acquisition, Writing – review & editing

HT: Conceptualisation, Supervision, Project Administration, Funding Acquisition, Writing – review & editing

TR: Conceptualisation, Supervision, Project Administration, Funding Acquisition, Writing – review & editing

DL: Investigation, Writing - review & editing

TT: Investigation, Writing - review & editing

ME: Investigation, Formal Analysis, Data Curation, Writing – review & editing

LB: Investigation, Writing - review & editing

SS: Writing - review & editing

HH: Writing - review & editing

https://doi.org/10.5194/ar-2026-32
Preprint. Discussion started: 22 September 2026

Acknowledgements

We thank Sami Jokelainen, Leena Stenlund, Piia Markkanen, Jouni Ahtiainen and the City of Vantaa for providing the premises for the Airport stationery site measurements as well as for other support. This work was done as a part of the GIANT-project (Global trends in IAQ: Novel technologies, Competence and Business), funded by Business Finland (5582/31/2023), participating companies, cities and municipalities. We want to thank Airmodus Oy, Airyn Oy, Dekati Oy and Pegasor Oy for the collaboration and their contributions during the campaign. The support from ACCC Flagship (grant nos. 337552 and 337551) is gratefully acknowledged. The NOAA Air Resources Laboratory (ARL) is acknowledged for providing the HYSPLIT transport and dispersion model and/or the READY website (https://www.ready.noaa.gov) used in this study. Paperpal AI tool was used to inspect the grammar of the manuscript.

Data availability

Data are available upon request from the corresponding author, Sami D. Harni (sami.harni@fmi.fi).

Supplement

Competing interests

At least one of the (co-)authors is a member of the editorial board of Atmospheric Chemistry and Physics.

References

Bucur, E., & Danet, A. (2019). Indoor/outdoor correlations regarding indoor air pollution with particulate matter. *Environmental Engineering and Management Journal*, *18*(2), 425–432. http://www.eemj.icpm.tuiasi.ro/;http://www.eemj.eu

Cappa, C. D., Lim, C. Y., Hagan, D. H., Coggon, M., Koss, A., Sekimoto, K., De Gouw, J., Onasch, T. B., Warneke, C., & Kroll, J. H. (2020). Biomass-burning-derived particles from a wide variety of fuels-Part 2: Effects of photochemical aging on particle optical and chemical properties. *Atmospheric Chemistry and Physics*, *20*(14), 8511–8532. https://doi.org/10.5194/acp-20-8511-2020

Colbeck, I., & Lazaridis, M. (2010). Aerosols and environmental pollution. *Naturwissenschaften*, *97*, 117–131. https://doi.org/10.1007/s00114-009-0594-x

Costabile, F., Gilardoni, S., Barnaba, F., Di Ianni, A., Di Liberto, L., Dionisi, D., Manigrasso, M., Paglione, M., Poluzzi, V., Rinaldi, M., Facchini, M. C., & Paolo Gobbi, G. P. (2017). Characteristics of brown carbon in the urban Po Valley atmosphere. *Atmospheric Chemistry and Physics*, *17*(1), 313–326. https://doi.org/10.5194/acp-17-313-2017

https://doi.org/10.5194/ar-2026-32
Preprint. Discussion started: 22 September 2026

Deng, G., Li, Z., Wang, Z., Gao, J., Xu, Z., Li, J., & Wang, Z. (2015). Indoor/outdoor relationship of PM2.5 concentration in typical buildings with and without air cleaning in Beijing. *Indoor and Built Environment*, *26*(1). https://doi.org/10.1177/1420326X15604349

Durdina, L., Brem, B. T., Setyan, A., Siegerist, F., Rindlisbacher, T., & Wang, J. (2017). Assessment of Particle Pollution from Jetliners: From Smoke Visibility to Nanoparticle Counting. *Environmental Science and Technology*, *51*(6), 3534–3541. https://doi.org/10.1021/acs.est.6b05801

Franck, U., Herbarth, O., Wehner, B., Wiedensohler, A., & Manjarrez, M. (2003). How do the indoor size distributions of airborne submicron and ultrafine particles in the absence of significant indoor sources depend on outdoor distributions? *Indoor Air*, *13*(2), 174–181. https://doi.org/10.1034/j.1600-0668.2003.00177.x

Garbarienė, I., Pauraitė, J., Pashneva, D., Minderytė, A., Sarka, K., Dudoitis, V., Davulienė, L., Gaspariūnas, M., Kovalevskij, V., Lingis, D., Bučinskas, L., Šapolaitė, J., Ežerinskis, Ž., Mainelis, G., Ovadnevaitė, J., Kecorius, S., Plauškaitė-Šukienė, K., & Byčenkienė, S. (2022). Indoor-outdoor relationship of submicron particulate matter in mechanically ventilated building: Chemical composition, sources and infiltration factor. *Building and Environment*, *222*. https://doi.org/10.1016/j.buildenv.2022.109429

Hanley, J. T., Ensor, D. S., Smith, D. D., & Sparks, L. E. (1994). Fractional Aerosol Filtration Efficiency of In-Duct Ventilation Air Cleaners. *Indoor Air*, *4*(3), 169–178. https://doi.org/10.1111/j.1600-0668.1994.t01-1-00005.x

Järvinen, A., Aitomaa, M., Rostedt, A., Keskinen, J., & Yli-Ojanperä, J. (2014). Calibration of the new electrical low pressure impactor (ELPI+). *Journal of Aerosol Science*, *69*, 150–159. https://doi.org/10.1016/j.jaerosci.2013.12.006

Jayne, J. T., Leard, D. C., Zhang, X., Davidovits, P., Smith, K. A., Kolb, C. E., & Worsnop, D. R. (2000). Development of an aerosol mass spectrometer for size and composition analysis of submicron particles. *Aerosol Science and Technology*, *33*(1–2), 49–70. https://doi.org/10.1080/027868200410840

Johnson, A. M., Waring, M. S., & DeCarlo, P. F. (2016). Real-time transformation of outdoor aerosol components upon transport indoors measured with aerosol mass spectrometry. *Indoor Air*, *27*(1), 230–240. https://doi.org/10.1111/ina.12299

Karjalainen, P., Saari, S., Kuuluvainen, H., Kalliohaka, T., Taipale, A., & Rönkkö, T. (2017). Performance of ventilation filtration technologies on characteristic traffic related aerosol down to nanocluster size. *Aerosol Science and Technology*, *51*(12), 1398–1408. https://doi.org/10.1080/02786826.2017.1356904

Kirchstetter, T. W., Novakov, T., & Hobbs, P. V. (2004). Evidence that the spectral dependence of light absorption by aerosols is affected by organic carbon. *Journal of Geophysical Research D: Atmospheres*, *109*(21). https://doi.org/10.1029/2004JD004999

Korhonen, Saija., Loukkola, K., & Portin, H. (2025). *Helsingin seudun ympäristöpalvelut-kuntayhtymä Samkommunen Helsingforsregionens miljötjänster Helsinki Region Environmental Services Authority*. www.hsy.fi

https://doi.org/10.5194/ar-2026-32
Preprint. Discussion started: 22 September 2026

Krebs, B., Burney, J., Zivin, J. G., & Neidell, M. (2021). Using Crowd-Sourced Data to Assess the Temporal and Spatial Relationship between Indoor and Outdoor Particulate Matter. *Environmental Science and Technology*, *55*(9), 6107–6115. https://doi.org/10.1021/acs.est.0c08469

Lepistö, T., Niemi, J. V., Salo, L., Silvonen, V., Elsayed, M., Jäppi, M., Stranden, T., Kylämäki, K., Harni, S. D., Sormunen, P., Manninen, H. E., Timonen, H., & Rönkkö, T. (2026). Dispersion of ultrafine particle pollution from an international airport: Characteristics and short- and long-term effects in surrounding areas. *Environment International*, *208*. https://doi.org/10.1016/j.envint.2026.110116

Li, B., Wang, M., Wang, D., Zhang, Q., Shi, L., Wei, X., Xue, W., & Jiang, J. (2026). Real-world aviation emissions of ultrafine particles and nitric oxide: The trade-off between fuel efficiency and pollutant emissions. *Atmospheric Environment*, *372*. https://doi.org/10.1016/j.atmosenv.2026.121897

Lintusaari, H., Kuuluvainen, H., Vanhanen, J., Salo, L., Portin, H., Järvinen, A., Juuti, P., Hietikko, R., Teinilä, K., Timonen, H., Niemi, J. V., & Rönkkö, T. (2023). Sub-23 nm Particles Dominate Non-Volatile Particle Number Emissions of Road Traffic. *Environmental Science and Technology*, *57*(29), 10763–10772. https://doi.org/10.1021/acs.est.3c03221

Liu, C., Chung, C. E., Yin, Y., & Schnaiter, M. (2018). The absorption Ångström exponent of black carbon: From numerical aspects. *Atmospheric Chemistry and Physics*, *18*(9), 6259–6273. https://doi.org/10.5194/acp-18-6259-2018

Lunden, M. M., Revzan, K. L., Fischer, M. L., Thatcher, T. L., Littlejohn, D., Hering, S. V., & Brown, N. J. (2003). The transformation of outdoor ammonium nitrate aerosols in the indoor environment. *Atmospheric Environment*, *37*(39–40), 5633–5644. https://doi.org/10.1016/j.atmosenv.2003.09.035

Masiol, M., Vu, T. V., Beddows, D. C. S., & Harrison, R. M. (2016). Source apportionment of wide range particle size spectra and black carbon collected at the airport of Venice (Italy). *Atmospheric Environment*, *139*, 56–74. https://doi.org/10.1016/j.atmosenv.2016.05.018

Matz, C. J., Stieb, D. M., Davis, K., Egyed, M., Rose, A., Chou, B., & Brion, O. (2014). Effects of age, season, gender and urban-rural status on time-activity: Canadian human activity pattern survey 2 (CHAPS 2). *International Journal of Environmental Research and Public Health*, *11*(2), 2108–2124. https://doi.org/10.3390/ijerph110202108

Miller, S. L., Facciola, N. A., Toohey, D., & Zhai, J. (2017). Ultrafine and fine particulate matter inside and outside of mechanically ventilated buildings. *International Journal of Environmental Research and Public Health*, *14*(2). https://doi.org/10.3390/ijerph14020128

Mohammadabadi, A., Skreiberg, Ø., & Georges, L. (2026). Heating habits and thermal comfort using wood stoves: a questionnaire-based analysis in Norway. *Energy and Built Environment*. https://doi.org/10.1016/j.enbenv.2026.05.009

Niemi, J. V., Saarikoski, S., Aurela, M., Tervahattu, H., Hillamo, R., Westphal, D. L., Aarnio, P., Koskentalo, T., Makkonen, U., Vehkamäki, H., & Kulmala, M. (2009). Long-range transport episodes of fine particles in southern Finland during 1999-2007. *Atmospheric Environment*, *43*(6), 1255–1264. https://doi.org/10.1016/j.atmosenv.2008.11.022

https://doi.org/10.5194/ar-2026-32
Preprint. Discussion started: 22 September 2026

Norra, S., Song, J., Gebhardt, R., Bauer, J., Broß, M., Fuchs, M., Huber, T., Mack, D., & Saathoff, H. (2023). Spatio-temporal dynamics of aerosol distribution in an urban environment recorded in situ by means of a bike based monitoring system. *Frontiers in Environmental Science*, *11*. https://doi.org/10.3389/fenvs.2023.749477

Olstrup, H., Hagenbjörk, A., & Orru, H. (2021). Ventilation systems and their impact on nanoparticle concentrations in office buildings. *Applied Sciences (Switzerland)*, *11*(19). https://doi.org/10.3390/app11198930

Onasch, T. B., Trimborn, A., Fortner, E. C., Jayne, J. T., Kok, G. L., Williams, L. R., Davidovits, P., & Worsnop, D. R. (2012). Soot particle aerosol mass spectrometer: Development, validation, and initial application. *Aerosol Science and Technology*, *46*(7), 804–817. https://doi.org/10.1080/02786826.2012.663948

Park, J. S., Jee, N. Y., & Jeong, J. W. (2014). Effects of types of ventilation system on indoor particle concentrations in residential buildings. *Indoor Air*, *24*(6), 629–638. https://doi.org/10.1111/ina.12117

Pauraite, J., Mainelis, G., Kecorius, S., Minderytė, A., Dudoitis, V., Garbarienė, I., Plauškaitė, K., Ovadnevaite, J., & Byčenkienė, S. (2021). Office indoor PM and BC level in Lithuania: The role of a long-range smoke transport event. *Atmosphere*, *12*(8). https://doi.org/10.3390/atmos12081047

Robinson, E. S., Gu, P., Ye, Q., Li, H. Z., Shah, R. U., Apte, J. S., Robinson, A. L., & Presto, A. A. (2018). Restaurant Impacts on Outdoor Air Quality: Elevated Organic Aerosol Mass from Restaurant Cooking with Neighborhood-Scale Plume Extents. *Environmental Science and Technology*, *52*(16), 9285–9294. https://doi.org/10.1021/acs.est.8b02654

Rumchev, K., Brown, H., & Spickett, J. (2007). Volatile organic compounds: Do they present a risk to our health? *Reviews on Environmental Health*, *22*(1), 39–56. https://doi.org/10.1515/REVEH.2007.22.1.39

Saksena, S., & Uma, R. (2008). Longitudinal study of indoor particulate matter and its relationship to outdoor concentrations in New Delhi, India. *Indoor and Built Environment*, *17*(6), 543–551. https://doi.org/10.1177/1420326X08097294

Sandradewi, J., Prévôt, A. S. H., Szidat, S., Perron, N., Alfarra, M. R., Lanz, V. A., Weingartner, E., & Baltensperger, U. R. S. (2008). Using aerosol light abosrption measurements for the quantitative determination of wood burning and traffic emission contribution to particulate matter. *Environmental Science and Technology*, *42*(9), 3316–3323. https://doi.org/10.1021/es702253m

Santiago, J. L., Rivas, E., Buccolieri, R., Martilli, A., Vivanco, M. G., Borge, R., Carlo, O. S., & Martín, F. (2022). Indoor-outdoor pollutant concentration modelling: a comprehensive urban air quality and exposure assessment. *Air Quality, Atmosphere and Health*, *15*, 1583–1608. https://doi.org/10.1007/s11869-022-01204-0

Sarnat, S. E., Coull, B. A., Ruiz, P. A., Koutrakis, P., & Suh, H. H. (2006). The Influences of Ambient Particle Composition and Size on Particle Infiltration in Los Angeles, CA, Residences. *Journal of the Air and Waste Management Association*, *56*(2), 186–196. https://doi.org/10.1080/10473289.2006.10464449

Shalini V., Gadag, G., & V Kalburgi, P. (2023). Atmospheric Aerosols and their Effect on Human Health: A Review. *Middle East Journal of Applied Science & Technology*, *6*(3), 1–10. https://doi.org/10.46431/mejast.2023.6301

https://doi.org/10.5194/ar-2026-32
Preprint. Discussion started: 22 September 2026

Sharma, S., Richard Leaitch, W., Huang, L., Veber, D., Kolonjari, F., Zhang, W., Hanna, S. J., Bertram, A. K., & Ogren, J. A. (2017). An evaluation of three methods for measuring black carbon in Alert, Canada. *Atmospheric Chemistry and Physics*, *17*(24), 15225–15243. https://doi.org/10.5194/acp-17-15225-2017

Stacey, B., Harrison, R. M., & Pope, F. (2020). Evaluation of ultrafine particle concentrations and size distributions at London Heathrow Airport. *Atmospheric Environment*, *222*. https://doi.org/10.1016/j.atmosenv.2019.117148

Takegawa, N. (2023). Field observations of aerosol particles in aircraft takeoff and taxiing plumes: A case study at Kobe Airport, Japan. *Aerosol Science and Technology*, *57*(11), 1087–1097. https://doi.org/10.1080/02786826.2023.2249069

Talbot, N., Kubelová, L., Makeš, O., Ondráček, J., Cusack, M., Schwarz, J., Vodička, P., Zíková, N., & Ždímal, V. (2017). Transformations of aerosol particles from an outdoor to indoor environment. *Aerosol and Air Quality Research*, *17*(3), 653–665. https://doi.org/10.4209/aaqr.2016.08.0355

Teinilä, K., Saarikoski, S., Lintusaari, H., Lepistö, T., Marjanen, P., Aurela, M., Hellén, H., Tykkä, T., Lampimäki, M., Lampilahti, J., Barreira, L., Mäkelä, T., Kangas, L., Hatakka, J., Harni, S., Kuula, J., Niemi, J. V., Portin, H., Yli-Ojanperä, J., … Timonen, H. (2025). Measurement report: Wintertime aerosol characterization at an urban traffic site in Helsinki, Finland. *Atmospheric Chemistry and Physics*, *25*(9), 4907–4928. https://doi.org/10.5194/acp-25-4907-2025

Timonen, H., Teinilä, K., Aurela, M., Reyes, F., Vásquez, Y., Bloss, M., Oyola, P., Hillamo, R., Asmi, E., & Saarikoski, S. (2018). Sources and composition of particulate matter in boreal arctic environment next to an active mining area. *Boreal Environment Research*, *23*, 105–125. www.tofwerk.com/tofware

Voigt, C., Märkl, R., Sauer, D., Dischl, R., Renard, C., Seeliger, K., Yu, F., Kaufmann, S., Bräuer, T., Jurkat-Witschas, T., Le Chenadec, G., Moreau, J., Requena-Esteban, E., Bonne, N., Vals, M., Roche, A., Zelina, J., Dörnbrack, A., Eirenschmalz, L., … Le Clercq, P. (2026). Substantial aircraft contrail formation at low soot emission levels. *Nature*, *652*, 112–118. https://doi.org/10.1038/s41586-026-10286-0

Vu, T. V., Zauli-Sajani, S., Poluzzi, V., Delgado-Saborit, J. M., & Harrison, R. M. (2017). Loss processes affecting submicrometer particles in a house heavily affected by road traffic emissions. *Aerosol Science and Technology*, *51*(10), 1201–1211. https://doi.org/10.1080/02786826.2017.1343453

Wu, T., & Boor, B. E. (2021). Urban aerosol size distributions: A global perspective. *Atmospheric Chemistry and Physics*, *21*(11), 8883–8914. https://doi.org/10.5194/acp-21-8883-2021

Yli-Tuomi, T., Lanki, T., Hoek, G., Brunekreef, B., & Pekkanen, J. (2008). Determination of the sources of indoor PM2.5 in Amsterdam and Helsinki. *Environmental Science and Technology*, *42*(12), 4440–4446. https://doi.org/10.1021/es0716655